



Perfect Absorber Based on Epsilon-Near-Zero Metamaterial as a Refractive Index Sensor

Behnoush Ghafari¹ · Mohammad Danaie¹ · Majid Afsahi¹

Received: 7 September 2022 / Revised: 30 April 2023 / Accepted: 8 May 2023 /
Published online: 22 May 2023

© The Author(s), under exclusive licence to Springer Science+Business Media, LLC, part of Springer Nature 2023

Abstract

We have designed a multilayer metamaterial structure which exploits the epsilon-near-zero (ENZ) mode for perfect absorption. The design procedure is based on the effective medium theory (EMT) model. The proposed multilayer structure consists of layers of Ag, InSb, SiO₂. The thickness of the layers is adjusted so that the ENZ mode is at the communication wavelength of 1550 nm. Two alternations of the layered structure are placed on a metal (Ag) substrate to prevent light transmission. Placing the nano-ring cavity arrays at the top of the multilayer structure leads to excitation of the surface plasmon polaritons (SPPs) and the cavity mode. Consequently, a resonance peak with nearly perfect absorption of 99.92% for normal incidence is obtained. Since the dimensions of the nano-ring affect the resonance wavelength, it is tuned to be exactly at the wavelength of the ENZ mode, resulting in perfect absorption. Simulation results based on the finite difference frequency domain method indicate that the absorption is insensitive to polarization and the absorption efficiency remains above 90% up to a 60° incident angle. The proposed absorber can be used for various optical communication applications such as filters, detectors and sensors. Finally, the structure's sensitivity to the environmental refractive index variations has been used here for refractive index sensing. A sensitivity of 200 nm/Refractive Index Unit (RIU) is obtained in this case.

Keywords Epsilon-near-zero · Metamaterial · Perfect absorber · Surface plasmons · Refractive index sensor

✉ Mohammad Danaie
danaie@semnan.ac.ir

¹ Faculty of Electrical and Computer Engineering, Semnan University, Semnan, Iran

1 Introduction

Generally, the metamaterial science aims to obtain materials with electrical and magnetic properties that are commonly not found or rarely found in nature [1, 2]. Since the parameters of electric permittivity and magnetic permeability are effective factors in the interaction of matter and light, by adjusting and modifying these parameters, new optical devices with unique features can be achieved [3]. One of the attractive applications of optical metamaterials is the perfect absorber [4]. Achieving perfect absorption typically requires materials with high optical losses, and high thicknesses. The use of metamaterial structure overcomes the mentioned limitations [5].

In recent years, a huge amount of research has been allocated to epsilon-near-zero materials (ENZ), which indicates attractive properties such as strong light-matter interaction and nanoscale field confinement [6, 7]. The real part of electric permittivity for ENZ materials is close to zero at certain frequencies. This phenomenon is naturally found in noble metals, polar dielectrics, doped semiconductors, and transparent conducting oxides [8, 9]. One of the easiest ways to obtain ENZ mode at the desired frequency is by alternating layers of a metal and a dielectric material. Since metals have a negative electric permittivity (below the plasma frequency), by placing a dielectric with a positive electric permittivity between metal layers and also by proper referring to the effective medium model, the ENZ mode can be achieved at the desired frequency [10]. The effective medium model is a homogenization method based on field averaging which is used to obtain the optical properties of the structure [11]. In the following, we will examine some epsilon near zero structures.

The most common and simplest method to obtain ENZ metamaterials is alternating dielectric-metal multilayer structures as used in [8, 12] for the visible wavelength range. In [13], metal (Ag) and semiconductor (Ge) alternating layers and in [14], dielectric (SiO₂) and semiconductor (InSb) alternating layers have been used to design ENZ metamaterials in the near-infrared spectrum. In [15], unlike conventional two-layer structures, a three-layer metal (Ag), dielectric (Al₂O₃) and semiconductor (Ge) structure is used, allowing more control in adjusting the ENZ wavelength over a wider range. In [16, 17], thin ITO layers are used to provide electrically tunable absorbers. Strong absorption modulation is achieved when the electrical permittivity is modified through an external electrical bias from a negative value to a positive value (ENZ mode). In [18], relying on the feature of increasing the interaction between light and ENZ material and also using coupling between ENZ mode and plasmon mode, strong broadband absorption in the infrared spectrum (>95%) has been observed. It is mentioned that the structure's potential applications are for solar energy harvesting, sensing and imaging. A dual-band refractive index biosensor with the ability to electrically adjust the ENZ wavelength by applying different voltages to the ITO is provided in [19]. The ENZ mode and the grating together excite the resonance, and an almost perfect absorption of 99.7% occurs at 1144 and 1404 nm.

The studying of ENZ materials and their properties is still an interesting and up-to-date topic. In this paper, we have designed a perfect absorber based on the

field confinement property of ENZ material with a thickness much less than the working wavelength. First, according to the EMT model, we adjust the thickness of the multilayer metamaterial layers so that the ENZ mode occurs at the desired wavelength of 1550 nm. By using it in the proposed absorber design and exciting the SPP and cavity mode at the same wavelength, the absorption efficiency of 99.92% is obtained. The absorption is insensitive to polarization and slightly sensitive to the angle of incidence, i.e., the absorption rate remains above 90% up to a 60-degree angle. This Absorber shows a sensitivity of 200 nm/refractive index unit (RIU) when changing the background's refractive index. It should be noted that all the simulations were performed using the hexahedral mesh analysis method and based on the finite difference frequency domain method of CST Microwave Studio software. The boundary condition settings in the x and y directions are periodic for the unit cell, and for the z direction the "open add space" boundary condition has been used. the electromagnetic waves are perpendicular to the z surface of the structure.

2 Structure Design Method

Figure 1a represents a schematic of an alternating multilayer metamaterial consisting of metal (Ag), semiconductor (InSb) and dielectric (SiO_2) materials with permittivities of ϵ_1 , ϵ_2 and ϵ_3 , respectively. The Drude model describes the permittivity of Ag and InSb as $\epsilon = \epsilon_\infty - \frac{\omega_p^2}{\omega^2 - i\gamma\omega}$. For Ag, the permittivity, the plasma frequency, and the collision frequency are $\epsilon_\infty = 5$, $\omega_p = 14 \times 10^{15}$ rad/s, and $\gamma = 2.01 \times 10^{14}$ rad/s and for InSb they are equal to $\epsilon_\infty = 15.68$, $\omega_p = 2.8 \times 10^{12}$ rad/s, and $\gamma = 0.3 \times 10^{12}$ rad/s [20, 21]. The permittivity of SiO_2 can be assumed as $\epsilon_3 = 3.8$. The thickness of the layers are equal to $h_1 = 10$ nm, $h_2 = 16$ nm and $h_3 = 20$ nm, respectively. Since the thickness of the layers is very small compared to the wavelength, the EMT model can be used to calculate the effective permittivity of the multilayer structure [22]:

$$\epsilon_{eff} = \epsilon_0 \begin{pmatrix} \epsilon_\perp & 0 & 0 \\ 0 & \epsilon_\perp & 0 \\ 0 & 0 & \epsilon_\parallel \end{pmatrix} \quad (1)$$

where, ϵ_\perp and ϵ_\parallel are the components perpendicular and parallel to the plane x-y, respectively.

$$\epsilon_\perp = \sum_j^{N_c} f_j \epsilon_j, j = 1, 2, 3 \quad (2)$$

$$\frac{1}{\epsilon_\parallel} = \sum_j^{N_c} f_j \frac{1}{\epsilon_j}, j = 1, 2, 3 \quad (3)$$

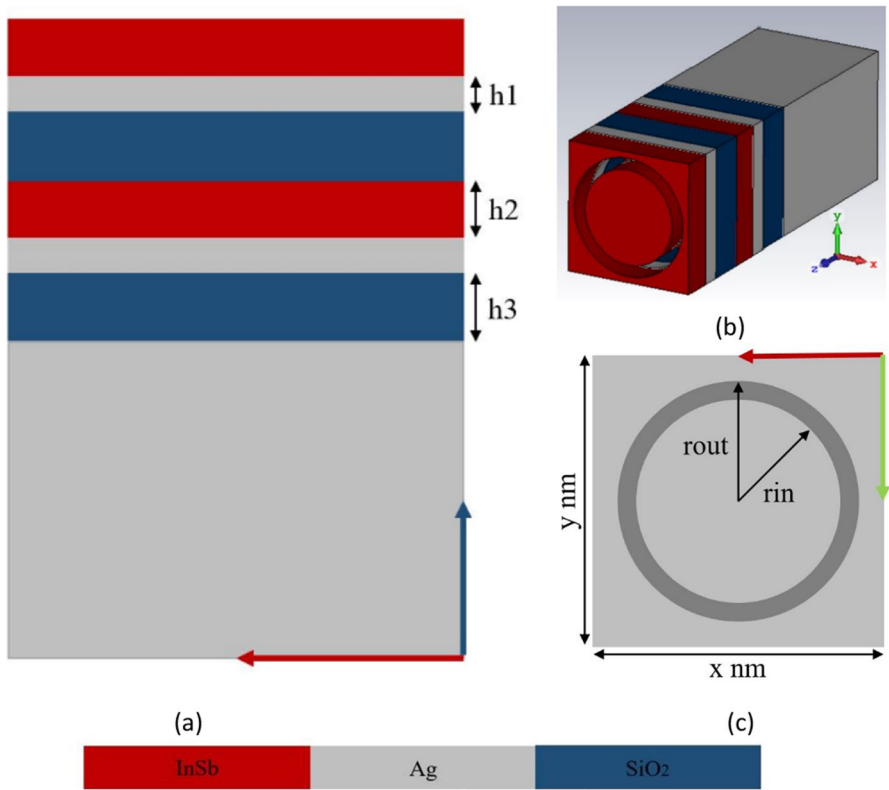
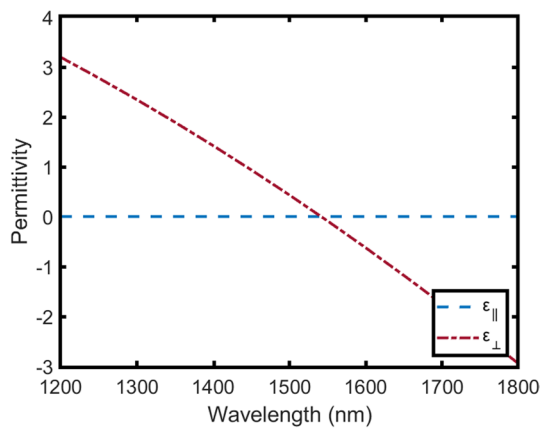


Fig. 1 **a** Schematic of a multilayer metamaterial consisting of InSb–Ag–SiO₂, **b** perfect absorber 3D view, and **c** top view

Fig. 2 Real parts of the effective permittivity tensor of the multilayer metamaterial



where, f_j and ϵ_j are the filling fractions and the permittivity of the j -layer [10]. As shown in Fig. 2, the thickness of the layers is adjusted so that the values of ϵ_{\perp} and ϵ_{\parallel} at a wavelength of 1550 nm are equal to zero. Consequently, it can be concluded that ϵ_{eff} is also equal to zero (Table 1).

Table 1 shows the parameters chosen in this structure. To further investigate the role of the thickness of each layer in determining the desired wavelength, by keeping the thickness of the two layers constant at the mentioned values, we only need to change the thickness of one layer and compare the results. In Figure 3a, by changing the thickness of h_1 from 6 to 14 nm with 2 nm steps, we see that increasing the thickness of the gold layer reduces the wavelength of the ENZ mode. In Figure 3b, c, by changing the thickness of h_2 from 8 to 24 nm with 4 nm steps and changing the thickness of h_3 from 5 to 25 nm with 5 nm steps, it can be seen that increasing the thickness of the InSb layer and SiO_2 increases the ENZ mode's wavelength. By examining the results, it can be seen that negative permittivity reduces the ENZ wavelength and positive permittivity increases the ENZ wavelength. It should be noted that changes in the thickness of gold can be much more effective and of higher sensitivity.

Next, by inserting the nano-ring cavity arrays on top of the multilayer metamaterial according to Figure 1b, c, the SPP and cavity mode [23] are excited (as used in [24]). ENZ excitation depends on the Brewster angle of the TM polarization or coupling with other modes [25, 26]. The dimensions of the nano-ring are designed so that the resonance occurs at the ENZ wavelength, which results in the coupling of the SPP and cavity modes with the ENZ mode. As indicated in Figure 4, the thin layers of metamaterials that support the ENZ mode strongly confine light and electric fields inside the sub-wavelength layers, resulting in perfect absorption (99.92%) [9, 27].

Figure 5 shows that by increasing the radius of the nano-ring (The width of the gap was constant, which means that the inner radius and the outer radius changed equally), the resonance frequency is shifted to higher wavelengths. The origin of this change can be explained by the LC equivalent circuit. The dielectric that covers the inside of the nano-ring cavity is considered a gap capacitor, which, according to the equation $C = \epsilon_0 \epsilon_r \sigma_{eff} / w$, where ϵ_0 is the permittivity of vacuum, ϵ_r is the relative permittivity of the nano-ring cavity or the same air here, σ_{eff} is the effective area, and w is wide of the nano-ring. Since the radius of the nano-ring is directly related to the effective area. An increase in the radius

Table 1 Structural parameters of the proposed absorber

Row	Parameter	Value (nm)
1	h_1 (Ag)	10
2	h_2 (InSb)	16
3	h_3 (SiO ₂)	20
4	rou _t	30
5	rin	26
6	$x \times y$	33×33

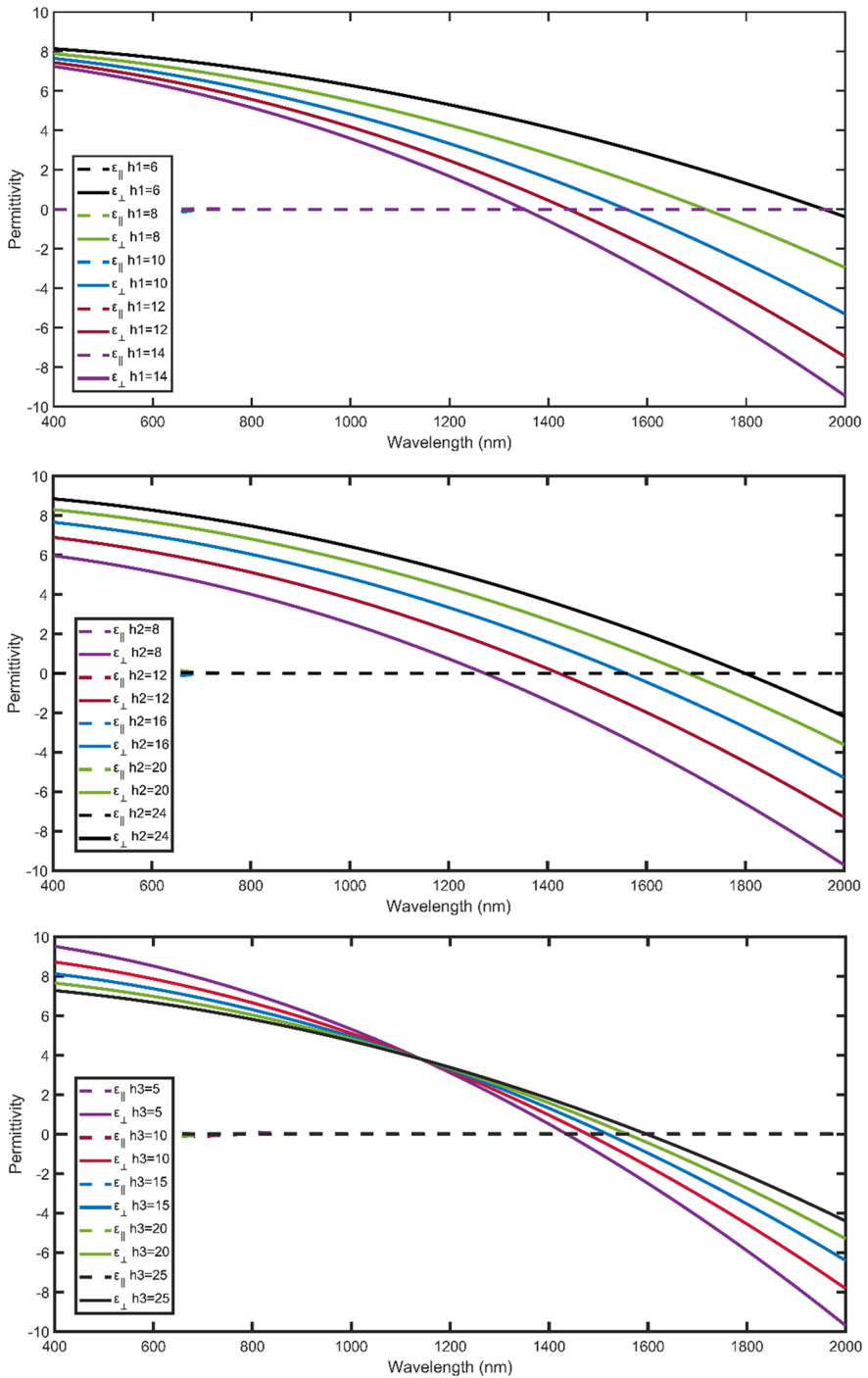


Fig. 3 Permittivity curves versus wavelength for different values of **a** h_1 , **b** h_2 and **c** h_3 and its effect on ENZ wavelength

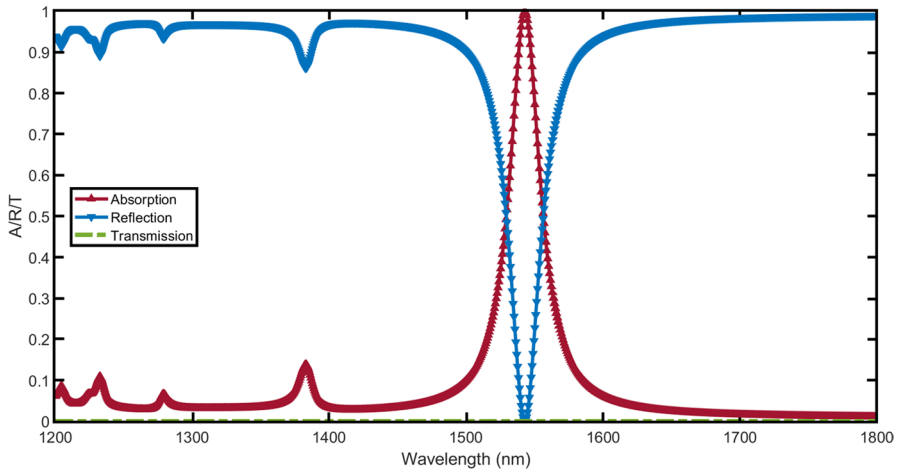


Fig. 4 Transmittance (T), reflectance (R), and absorption (A) for the proposed absorber based on ENZ metamaterial

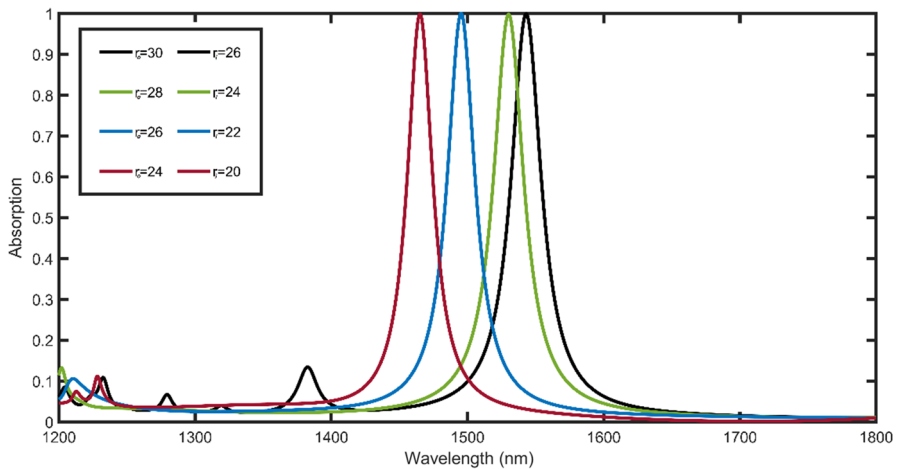


Fig. 5 Normalized absorption versus radius of nano-ring and its effect on resonance wavelength

causes an increase in the value of the gap capacitor, which also increases the resonance wavelength [28]. The study of layer thickness changes and nano-rings is needed to be able to design the structure at other wavelengths.

Regarding the proposed absorber construction, it should be mentioned that this process consists of two steps, i.e., the deposition of thin layers on the substrate by using Ion-beam Sputter Deposition (IBSD) methods, and the insertion of the nano-ring cavity arrays by the focused ion beam-scanning electron

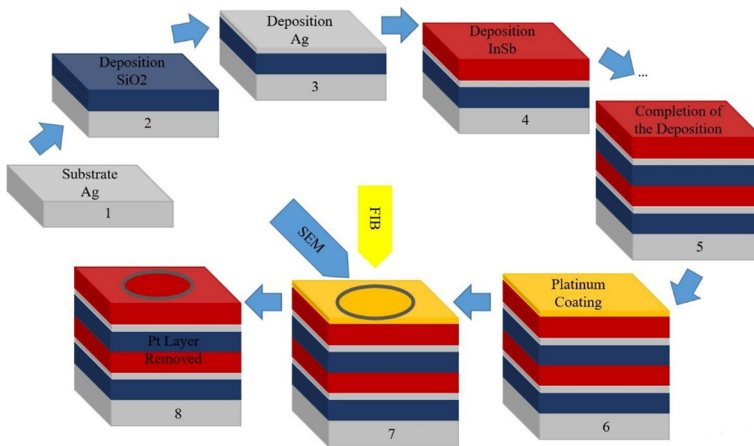


Fig. 6 Schematic of the manufacturing process

microscope (FIB-SEM) [29–31]. A schematic of the manufacturing process is given in Figure 6.

3 Results and Discussions

As shown in Figure 7, absorption is obtained at two polarizations (TM and TE), at different incident angles. The results clearly show that the absorption is insensitive to polarization and sensitive to the incident angle. Fortunately, the absorption rate remains above 90% up to a 60-degree angle, but at a 90-degree angle, the absorption is almost zero. The incident angle of EM wave affects impedance matching, and designing structures with symmetry only increases the angular range of insensitivity of the structure [32–34].

As was said before, the thickness of the layers determines the ENZ wavelength, as the angle of incidence increases, the effective thickness for the incident wavelength increases, and the ENZ wavelength shifts. This displacement causes weak coupling or even no coupling of the ENZ mode with other modes and decreases absorption intensity.

The electric field distributions are shown in Figure 8a, b at the 1550 nm resonance wavelength for TM and TE polarizations, respectively. According to the figure, it can be seen that the maximum E-field appears at the boundary between metal-dielectric and metal-semiconductor, which shows that the resonance absorption peak is mainly due to the excitation of the SPPs. In addition, part of the E-field is trapped in the nano-ring cavity.

Due to the Absorber's sensitivity to the environment's refractive index, one of its potential applications is as a refractive index sensor. As shown in Fig. 9, by changing the refractive index of the medium with steps of 0.05, the wavelength changes by about 10 nm. According to the definition of sensitivity [35], $S = \frac{\Delta\lambda(\text{Peak})}{\Delta n} \left[\frac{\text{nm}}{\text{RIU}} \right]$, the sensitivity of this sensor is 200 nm/RIU. The figure of

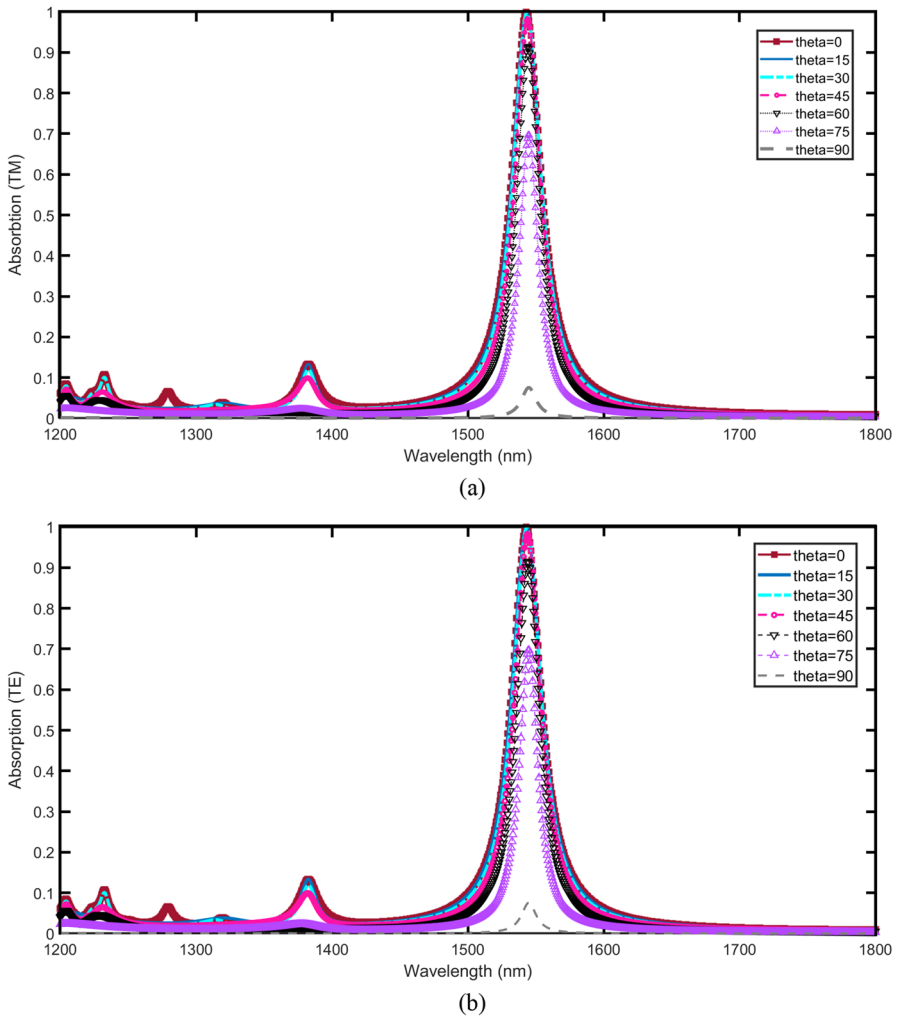


Fig. 7 Absorption spectra for different incident angles: **a** TM polarization and **b** TE polarization

merit (FOM) relation is also equal to $FOM = \frac{S}{FWHM_{Bandwidth}}$. Since the full width at half maximum (FWHM) bandwidth is equal to 27, the FOM value is 7.4. By increasing the refractive index and moving away from the ENZ wavelength, the absorption rate has decreased. In addition to various applications of absorbers at a telecommunication wavelength of 1550 nm, this structure can also be used in refractive index sensing applications such as detecting liquids, gases, etc.

Given that the proposed structure is a perfect absorber, a comparison between its parameters and other works performed in this field is provided in Table 2. The comparison shows that this method provides a nearly perfect absorption,

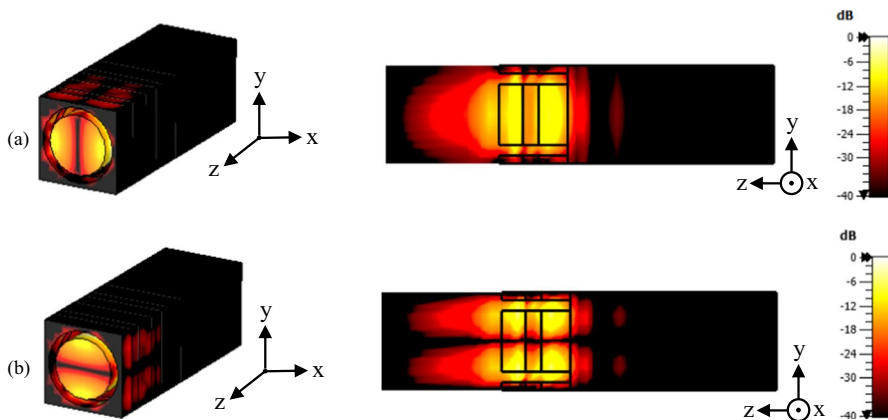


Fig. 8 E-field distributions of ENZ metamaterials in 3D & y - z -plane for **a** TM and **b** TE polarization

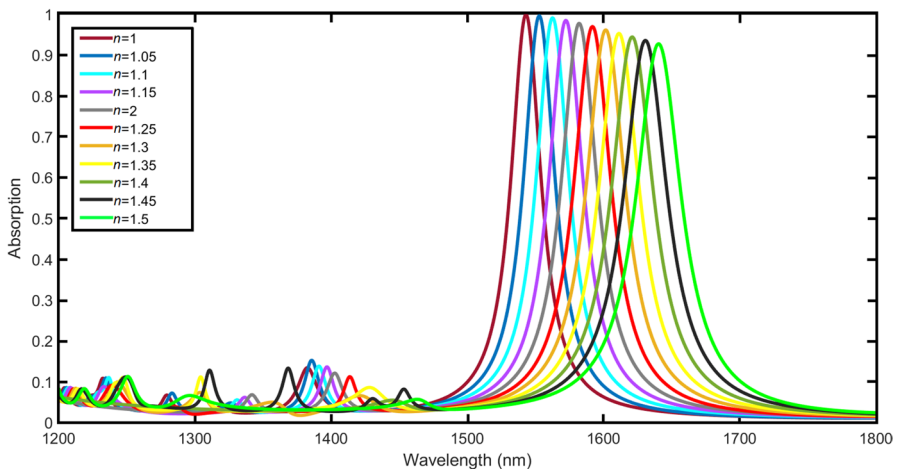


Fig. 9 The relationship of the medium refractive index with the absorption spectrum

while it is polarization insensitive and also the absorption peak is dedicated to the widely used telecommunication wavelength of 1550 nm.

4 Conclusion

A perfect absorber based on the ENZ metamaterial structure was presented. Placing the nano-ring cavity arrays at the top of the multilayer structure led to excitation of the SPPs and the cavity mode. Consequently, a resonance peak with nearly perfect absorption of 99.92% for 1550 nm at normal incidence was obtained. The proposed structure can detect changes in the refractive index of the environment and can be

Table 2 Comparison between the obtained results and the results recently reported in the literature

References	Year	Absorption wave-lengths (nm)	Absorption peaks	Polarization sensitivity	Incident angle sensitivity
[36]	2021	1310 1550	99.986% 99.421%	Polarization-independent	Insensitive to incident angle
[37]	2021	1550	Nearly 100%	Polarization-insensitive	Sensitive to the incident angle
[38]	2020	1550	99.99%	Insensitive to polarization	Insensitive to the angle of incidence
[32]	2020	955	99.8%	Independent of polarization	Independent of polarization angle
[39]	2020	1455.49	Higher than 99%	Sensitive to polarization (only TE)	Insensitive to incident angle
This work	–	1550	99.92%	Polarization-insensitive	Sensitive to the incident angle

used as a refractive index sensor. The sensitivity is $200 \text{ nm}/RIU$ and FOM is 7.4. More importantly, it should be mentioned that since the absorber works at a wavelength of 1550 nm, it can be used in other applications such as switching, filters, detectors, etc.

Author Contribution Design, analysis, and investigation: BG, Writing—original draft preparation: BG, Writing—review and editing: MD, Supervision: MD, MA.

Funding The authors declare that no funds, grants, or other support were received during the preparation of this manuscript.

Data Availability The datasets generated and analyzed during the current study are available from the corresponding author on reasonable request.

Declarations

Conflict of interest The authors declare no conflict of interests. The authors also have no relevant financial or non-financial interests to disclose.

Consent to Participate Not applicable

Consent to Publish Not applicable.

Ethical Approval We the undersigned declare that the manuscript entitled “Perfect Absorber Based on Epsilon-Near-Zero Metamaterial as a Refractive Index Sensor” is original, has not been fully or partly published before, and is not currently being considered for publication elsewhere. Also, results are presented clearly, honestly, and without fabrication, falsification, or inappropriate data manipulation. We confirm that the manuscript has been read and approved by all named authors and that there are no other persons who satisfied the criteria for authorship but are not listed. We further confirm that the order of authors listed in the manuscript has been approved by all of us.

References

1. Ciallella, A. (2020). Research perspective on multiphysics and multiscale materials: A paradigmatic case. *Continuum Mechanics and Thermodynamics*, 32(3), 527–539.
2. Nickpay, M. R., Danaie, M., & Shahzadi, A. (2022). Design of a graphene-based multi-band metamaterial perfect absorber in THz frequency region for refractive index sensing. *Physica E: Low-dimensional Systems and Nanostructures*, 138, 115114.
3. Yu, P., Besteiro, L. V., Wu, J., Huang, Y., Wang, Y., Govorov, A. O., & Wang, Z. (2018). Metamaterial perfect absorber with unabated size-independent absorption. *Optics Express*, 26(16), 20471–20480.
4. Liu, X., Li, K., Meng, Z., Zhang, Z., & Wei, Z. (2021). Hybrid metamaterials perfect absorber and sensitive sensor in optical communication band. *Frontiers in Physics*, 53.
5. Anopchenko, A., Tao, L., & Lee, H. W. H. (2017, July). Field-effect tunable epsilon-near-zero perfect absorbers. In 2017 Conference on Lasers and Electro-Optics Pacific Rim (CLEO-PR) (pp. 1–2). IEEE.
6. Johns, B., Chattopadhyay, S., & Mitra, J. (2022). Tailoring infrared absorption and thermal emission with ultrathin film interferences in epsilon-near-zero media. *Advanced Photonics Research*, 3(1), 2100153.
7. Sakotic, Z., Krasnok, A., Cselyuska, N., Jankovic, N., & Alú, A. (2020). Berreman embedded eigenstates for narrow-band absorption and thermal emission. *Physical Review Applied*, 13(6), 064073.

8. Gao, J., Sun, L., Deng, H., Mathai, C. J., Gangopadhyay, S., & Yang, X. (2013). Experimental realization of epsilon-near-zero metamaterial slabs with metal-dielectric multilayers. *Applied Physics Letters*, *103*(5), 051111.
9. Newman, W. D., Cortes, C. L., Atkinson, J., Pramanik, S., DeCorby, R. G., & Jacob, Z. (2015). Ferrell-Berremann modes in plasmonic epsilon-near-zero media. *ACS Photonics*, *2*(1), 2–7.
10. Shankhwar, N., & Sinha, R. K. (2021). Zero index metamaterials: Trends and applications. Springer Nature
11. Orlov, A. A., Voroshilov, P. M., Belov, P. A., & Kivshar, Y. S. (2011). Engineered optical nonlocality in nanostructured metamaterials. *Physical Review B*, *84*(4), 045424.
12. Subramania, G., Fischer, A. J., & Luk, T. S. (2012). Optical properties of metal-dielectric based epsilon near zero metamaterials. *Applied Physics Letters*, *101*(24), 241107.
13. Yang, X., Hu, C., Deng, H., Rosenmann, D., Czaplowski, D. A., & Gao, J. (2013). Experimental demonstration of near-infrared epsilon-near-zero multilayer metamaterial slabs. *Optics Express*, *21*(20), 23631–23639.
14. Cheng, C., Lu, Y., Zhang, D., Ruan, F., & Li, G. (2020). Gain enhancement of terahertz patch antennas by coating epsilon-near-zero metamaterials. *Superlattices and Microstructures*, *139*, 106390.
15. Vafaei, M., Moradi, M., & Bordbar, G. H. (2019). Realization of epsilon-near-zero metamaterial stack based on dielectric-semiconductor-metal multilayers. *Plasmonics*, *14*(6), 1929–1937.
16. Park, J., Kang, J. H., Liu, X., & Brongersma, M. L. (2015). Electrically tunable epsilon-near-zero (ENZ) metafilm absorbers. *Scientific reports*, *5*(1), 1–9.
17. Wang, Z., Zhou, P., & Zheng, G. (2019). Electrically switchable highly efficient epsilon-near-zero metasurfaces absorber with broadband response. *Results in Physics*, *14*, 102376.
18. Dang, P. T., Le, K. Q., Lee, J. H., & Nguyen, T. K. (2019). A designed broadband absorber based on ENZ mode incorporating plasmonic metasurfaces. *Micromachines*, *10*(10), 673.
19. Meng, Z., Cao, H., Liu, R., & Wu, X. (2020). An electrically tunable dual-wavelength refractive index sensor based on a metagrating structure integrating epsilon-near-zero materials. *Sensors*, *20*(8), 2301.
20. Rahmatiyar, M., Afsahi, M., & Danaie, M. (2020). Design of a refractive index plasmonic sensor based on a ring resonator coupled to a MIM waveguide containing tapered defects. *Plasmonics*, *15*(6), 2169–2176.
21. Howells, S. C., & Schlie, L. A. (1996). Transient terahertz reflection spectroscopy of undoped InSb from 0.1 to 1.1 THz. *Applied Physics Letters*, *69*(4), 550–552.
22. Guo, Z., Jiang, H., & Chen, H. (2020). Hyperbolic metamaterials: From dispersion manipulation to applications. *Journal of Applied Physics*, *127*(7), 071101.
23. Jafari, D., Danaie, M., Rezaei, P., & Nurmohammadi, T. (2021). A novel variable-length header extraction scheme based on ring laser for all-optical packet switching network. *Optical and Quantum Electronics*, *53*(6), 1–9.
24. Mandal, P. (2021). Polarization insensitive plasmonic stacked multilayer metasurface with deep nanohole cavity as multi-band absorber. *Optik*, *241*, 166959.
25. Brener, I., & Marquier, F. (2014). Theory of Epsilon-Near-Zero Modes in Thin Films (No. SAND2014–20631C). Sandia National Lab.(SNL-NM), Albuquerque, NM (United States).
26. Bruno, V., Vezzoli, S., DeVault, C., Roger, T., Ferrera, M., Boltasseva, A., & Faccio, D. (2020). Dynamical control of broadband coherent absorption in ENZ films. *Micromachines*, *11*(1), 110.
27. Runnerstrom, E. L., Kelley, K. P., Folland, T. G., Nolen, J. R., Engheta, N., Caldwell, J. D., & Maria, J. P. (2018). Polaritonic hybrid-epsilon-near-zero modes: Beating the plasmonic confinement vs propagation-length trade-off with doped cadmium oxide bilayers. *Nano Letters*, *19*(2), 948–957.
28. Liu, F., Zou, M., Feng, Z., Ni, B., Ye, B., & Wang, Y. (2023). All-Dielectric Dual-Band Metamaterial Absorber Based on Ring Nanocavity in Visible Region for Sensing Applications. In *Photonics* (Vol. 10, No. 1, p. 58). Multidisciplinary Digital Publishing Institute.
29. Khan, Y., Butt, M. A., Kazanskiy, N. L., & Khonina, S. N. (2022). Numerical study of fabrication-related effects of the structural-profile on the performance of a dielectric photonic crystal-based fluid sensor. *Materials*, *15*(9), 3277.
30. Kannegulla, A., & Cheng, L. J. (2016). Metal assisted focused-ion beam nanopatterning. *Nanotechnology*, *27*(36), 36LT01

31. Khan, Y., Rehman, A. U., Batool, B. A., Noor, M., Butt, M. A., Kazanskiy, N. L., & Khonina, S. N. (2022). Fabrication and investigation of spectral properties of a dielectric slab waveguide photonic crystal based fano-filter. *Crystals*, *12*(2), 226.
32. Wu, P., Chen, Z., Jile, H., Zhang, C., Xu, D., & Lv, L. (2020). An infrared perfect absorber based on metal-dielectric-metal multi-layer films with nanocircle holes arrays. *Results in Physics*, *16*, 102952.
33. Hoa, N. T. Q., Tung, P. D., Dung, N. D., Nguyen, H., & Tuan, T. S. (2019). Numerical study of a wide incident angle-and polarisation-insensitive microwave metamaterial absorber based on a symmetric flower structure. *AIP Advances*, *9*(6), 065318.
34. Zhou, Q., Ma, W., Wu, T., Li, Y., Qiu, Q., Duan, J., & Huang, Z. (2022). Metasurface terahertz perfect absorber with strong multi-frequency selectivity. *ACS Omega*, *7*(41), 36712–36727.
35. Nohoji, A. H. A., & Danaie, M. (2022). Highly sensitive refractive index sensor based on photonic crystal ring resonators nested in a mach-zehnder interferometer
36. Liu, X., Li, K., Meng, Z., Zhang, Z., & Wei, Z. (2021). Hybrid metamaterials perfect absorber and sensitive sensor in optical communication band. *Frontiers in Physics*, *9*, 637602.
37. Meng, Q., Chen, X., Xu, W., Zhu, Z., Qin, S., Zhang, J., & Yuan, X. (2021). High Q resonant graphene absorber with lossless phase change material Sb₂S₃. *Nanomaterials*, *11*(11), 2820.
38. Ali, W., Iqbal, S., Ullah, M., & Wang, X. (2022). An ultrahigh narrowband absorber close to the information communication window. *Plasmonics*, *17*(2), 709–715.
39. Liao, Y. L., & Zhao, Y. (2020). Ultra-narrowband dielectric metamaterial absorber for sensing based on cavity-coupled phase resonance. *Results in Physics*, *17*, 103072.

Publisher's Note Springer Nature remains neutral with regard to jurisdictional claims in published maps and institutional affiliations.

Springer Nature or its licensor (e.g. a society or other partner) holds exclusive rights to this article under a publishing agreement with the author(s) or other rightsholder(s); author self-archiving of the accepted manuscript version of this article is solely governed by the terms of such publishing agreement and applicable law.